Correlation effects for highly Cr doped ZnSe

2007 J. Phys.: Condens. Matter 19 466209

(http://iopscience.iop.org/0953-8984/19/46/466209)

IOP PUBLISHING JOURNAL OF PHYSICS: CONDENSED MATTER

J. Phys.: Condens. Matter **19** (2007) 466209 (12pp) doi:10.1088/0953-8984/19/46/466209

Correlation effects for highly Cr doped ZnSe

C Tablero

Instituto de Energía Solar, Universidad Politécnica de Madrid, Ciudad Universitaria s/n, 28040 Madrid, Spain

Received 5 September 2007, in final form 5 October 2007
Published 23 October 2007
Online at stacks.iop.org/JPhysCM/19/466209

Abstract

A study of the electronic properties and correlation effects of Cr in ZnSe using first principles is presented. These materials have potential technological applications for mid-infrared lasers, solar cells and spintronics. They have an intermediate band in the host semiconductor band gap with the Fermi energy located within this intermediate band for a sufficiently high density of Cr substituting the Zn atoms. An analysis of the electronic properties is carried out using the local density approximation with a Hubbard term to improve the description of this intermediate band. The main effects when the Hubbard term is included are an increase in the bandwidth and the modification of the relative composition of the d and p Cr transition metal orbitals. From the results, the intermediate band is not split, creating two bands, for the Hubbard term between 0 and 9 eV. The relaxing of the atomic configurations causes a slight increase in the intermediate bandwidth and a decrease in the gaps. The effect of the correlation is lower than for other zinc chalcogenides doped with Cr.

(Some figures in this article are in colour only in the electronic version)

1. Introduction

Solid-state lasers operating in the mid-infrared spectral region are of interest for a wide variety of applications. The absorption and emission properties of transition metal doped zinc chalcogenides have been researched to understand their potential application as room-temperature, mid-infrared tunable laser media [1]. Cr is a highly favorable laser when it is incorporated into the zinc chalcogenides. The demonstration of lasing for Cr doped semiconducting ZnSe with a high quantum yield at room temperature has been carried out [1]. In contrast to other transition metal atoms, the Cr experiences very low non-radiative decay in the ZnSe host, and the emission cross section is very large. For a sufficiently high density of Cr substituting the Zn atoms these materials have the electronic structure of an intermediate band material. These materials have an intermediate band (IB) sandwiched between the valence (VB) and conduction band (CB) of the host semiconductor which, in a formal band-theoretic picture, is metallic because the Fermi energy is located within the intermediate band. This

basic electronic band structure is a characteristic of transparent conducting oxides, up- and down-converters and intermediate band solar cells. The electronic properties of intermediate band materials have also attracted a great deal of attention [2] within the photovoltaic field, where these types of materials could revolutionize modern solar cells because solar cells based on these materials can reach efficiencies higher than those of single-gap solar cells (63.17% [3] versus 40.7% [4]).

One useful approach to obtaining and understanding the electronic properties of these materials is the first-principles electronic approach. However, there are two big limitations. One limitation of this approach is the size of the system that can be handled. To model transition metal impurities in semiconductors, a large cell, the bigger the cell the smaller the metal concentration, needs to be used. The computational cost increases so much that it is not possible to obtain the lower concentration limit where the impurity atom introduces an isolated level into the band gap of the semiconductor. The IB will be formed when the impurity-induced levels broaden to make a band which is split off from the host semiconductor bands and lies in the band gap. The doping concentrations in this case will be bigger and can be modeled approximately using first-principles calculations, although the computational cost continues to be extremely high.

Another limitation is related to the properties of the IB: small bandwidth compared with the gap of the host semiconductor and partially full. Therefore, the local correlation effects are very important. Correlation effects are essentially the corrections to monoelectronic models. The correlation energy is usually defined as the part of the energy which is ignored when a monoelectronic theory is used. Therefore, a part of the so-called exchange energy is correlation energy, and it is not considered as a part of the so-called electron correlation energy. We will use the term correlation in a general sense. In particular, the self-interaction (a part of the so-called exchange energy) will be considered as correlation in a general sense. Unfortunately, these effects are ill described with methods based on density functional theory (DFT) [5, 6] in the local spin density approximation (LSDA). The main limitation of other, more sophisticated, methods [6], such as those based on Green functions with screened interaction (GW) and the exact exchange Kohn–Sham formalism (EXX), is that they are currently prohibitively expensive for large cells. At an intermediate level, the combination of LSDA with a Hubbard term (U) greatly improves the description of the localized states. The LSDA + U [7] method has been applied in a few systems [8–10]. The main effects of the LSDA + U corrections are an increase in the localization of the transition metal orbitals, a modification of the relative composition of the five transition metal d orbitals and a shift of the occupied and unoccupied d bands to lower and higher energies respectively.

Because of the IB characteristics, narrow and partially filled, it could split into two sub-bands, a full one and an empty one. Two possible factors are analyzed in this work: a lattice distortion and the strong Coulomb repulsion. In either one of the two cases, lattice distortion or strong Coulomb repulsion, we would not have a partially filled IB anymore, but two bands, a full one and an empty one. This would reduce the application of these materials because of the increase of the non-radiative transitions and the inhibition of the metallic conduction. In this paper we analyze these two factors using *ab initio* calculations for a material derived from the ZnSe host semiconductor where the Cr is incorporated by substituting the host metallic atom (one Cr for each of the 32 Zn atoms).

2. Calculations

The electronic structure calculations were carried out by using the LSDA method based on pseudopotentials for core electrons, and numerically localized pseudoatomic orbitals as the

basis set for the valence wavefunctions. The standard Kohn–Sham (KS) [11] equations are solved self-consistently [12]. For the exchange and correlation term, the LSDA has been used as proposed by Ceperley–Alder [13]. The standard Troullier–Martins [14] pseudopotential is adopted and expressed in the Kleinman–Bylander [15] factorization. The KS orbitals are represented using a linear combination of confined pseudoatomic orbitals [16]. The range of each orbital is determined by an orbital energy confinement of 0.01 Ryd. An analysis of the basis set convergence has also been carried out using from single-ζ to double-ζ with polarization basis sets for all atoms and varying the number of the special k points in the irreducible Brillouin zone. In all calculations a double-ζ with polarization functions basis set (DZP) has been used (two 4s and 3d shells plus a 3p polarization shell for Cr and Zn and two 4s and 4p shells plus a 4d polarization shell for Se), and we use periodic boundary conditions with 18 (four) special k points in the irreducible Brillouin zone (BZ) for a 64-atom (216-atom) cell.

For almost all calculations the zinc-blende ZnSe experimental lattice constant of 5.67 Å has been assumed. Nevertheless, in order to analyze whether a distortion splits the occupied and empty IB states, the cell-internal atom positions were allowed to relax in accordance with the calculated quantum mechanical forces (with no symmetry constraints) until the total energy minimum was reached and the forces became smaller than 0.004 eV Å^{-1}.

Because of the LSDA limitations, a further extension is carried out using the LSDA + U method, that greatly improves the description of the localized states of the IB. The LSDA + U method has been applied to similar systems [8–10] using the same calculation methodology [8, 9]. In the approach used [7] the double-counting correction term is given by the fully localized limit (FLL-LSDA + U). We assumed that the screened Coulomb and exchange parameters U and J are independent of the magnetic quantum number, although they are dependent on the quantum number l. In this system, with an isolated, partially filled IB for a spin channel, the interactions in like-spin and unlike-spin channels are small and the results are very insensitive to J when $U - J$ is fixed. Therefore, the onsite Coulomb term U, and the exchange term J, can always be grouped together into a single effective parameter $(U - J)$, and this effective parameter will simply be referred to as U in this paper. These approximations are equivalent to neglecting the possible non-spherical character of the effective interactions and the differences among the interactions in like-spin and unlike-spin channels (described by J). The electron potential used is the conventional LSDA plus an orbital dependent shift. These additional shifts of potential can be represented as a non-local potential $V_{\text{LDA}+U} = |m\rangle V_{\text{m}}^{(\sigma)} \langle m|$ where $V_{\text{m}}^{(\sigma)} = U(1/2 - n_{\text{m}}^{(\sigma)})$ and $n_{\text{m}}^{(\sigma)}$ is the occupation of the $|m\rangle$ orbital with spin σ: $n_{\text{m}}^{(\sigma)} = \langle m|[\sum_i |\varphi_i^{(\sigma)}\rangle f_i \langle \varphi_i^{(\sigma)}|]|m\rangle$ ($\varphi_i^{(\sigma)}$ are the Kohn–Sham states and f_i are the band occupations). This choice corresponds to the so-called *full* version of the occupation matrices and projectors.

3. Results and discussion

The system has been modeled using a unit cell with 64 atoms and periodic boundary conditions. This initial 64-atom cell (without relaxing) is derived from the ZnSe host semiconductor. In this structure, the Se atoms can be broken down into two groups: those directly bonded to the Cr atoms (four Se_1) and those which are not (28 Se_2). The atomic environment for each of the atoms is 4Se_1 for Cr, Cr + 3Zn for Se_1 and 4Zn for Se_2.

The energy band diagram in some directions of the BZ is shown in figure 1 with $U = 0$ eV. An isolated IB, made up of the majority spin component, appears between one full band (VB) and the empty band (CB). The Fermi energy (horizontal line in the figure) cuts this IB, showing

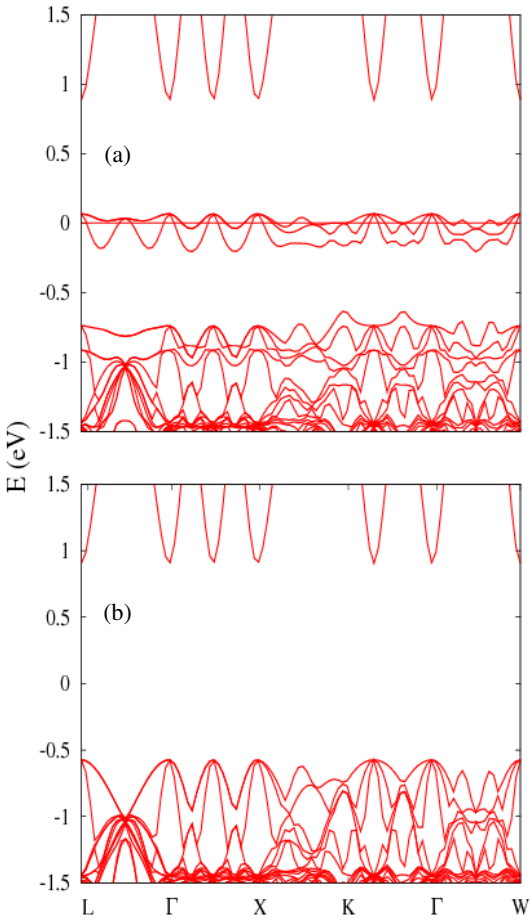

Figure 1. Energy bands (eV) in the principal directions of the Brillouin zone: (a) spin up, (b) spin down. The horizontal line in (a) is the Fermi energy (E_F) and it has been chosen as zero in this figure.

that the band is partially full. In order to identify the orbital composition of these bands the projected densities of states (DOS) of the Cr t(d_{xy}, d_{xz} and d_{yz}), e(d_{z^2} and $d_{x^2-y^2}$) and p orbitals are represented in figure 2. We see that the bands near the Fermi energy are t bands in all cases with a small contribution of Cr p orbitals. Therefore, the IB is made up mainly for the combination of the Cr t orbitals with the Se_1 p orbitals, also of t symmetry.

Jahn–Teller lattice distortion can occur because the triplet t majority spin bands are partially occupied by two electrons. In order to analyze whether a distortion splits the occupied and empty IB states, the cell-internal atom positions were allowed to relax. The fully relaxed atomic distances Cr–Se are bigger than the distances Zn–Se of the host semiconductor (2.46 Å): there are two distances the same (2.56 Å) and two different ones (2.48 and 2.55 Å); the local tetrahedral symmetry considering the immediate neighbors is slightly reduced to D_{2d}. The relaxing of the atomic configurations causes a downward shift of the IB, but a distortion driven by atomic relaxing that splits the occupied and empty IB states is not seen.

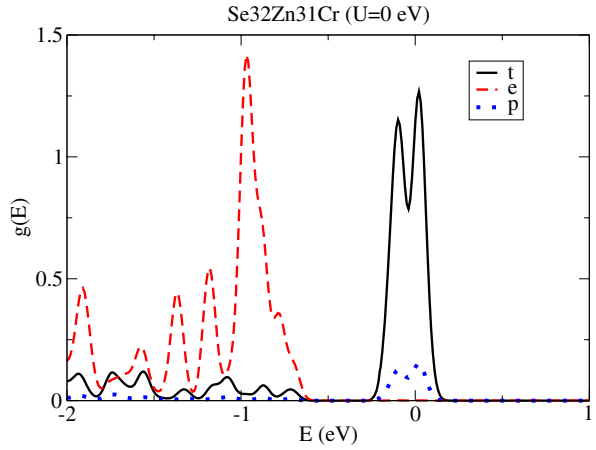

Figure 2. Projected spin up DOS on the Cr t, e and p orbitals. The Fermi energy has been chosen as zero in this figure.

Table 1. Mulliken population analysis of the Cr, Se and Zn atoms. The spin component is shown in the second column: + for majority and − for minority spin respectively. In the table Q is the atomic charge. The Se_1 atoms are those directly bonded to the Cr atom and the Se_2 atoms are those which are not.

Atom	Spin	Q	s	t	e	p
Cr	+	5.32	0.40	0.83	0.97	0.17
Cr	−	0.92	0.35	0.06	0.02	0.12
Se_1	+	3.00	0.85	0.01	0.01	0.70
Se_1	−	3.09	0.86	0.01	0.01	0.72
Se_2	+	3.08	0.87	0.01	0.01	0.71
Se_2	−	3.09	0.87	0.01	0.01	0.72
Zn	+	5.92	0.47	0.98	0.98	0.17
Zn	−	5.91	0.46	0.99	0.98	0.17

In order to analyze whether the IB is created within the band gap for a different concentration, we have also carried out a study with a unit cell with 216 host atoms where one Cr atom is substituted for each of the 108 Zn atoms. In this case the IB is also present.

To analyze the charge distribution in the system, the Mulliken population of the Cr, Se and Zn atoms is shown in table 1. It can be seen that the Cr d orbitals that have more charge associated are, in decreasing order, the e and t orbitals. The Se atom with the lower charge corresponds to Se_1 atoms bonded with Cr. The polarization of the Se atoms has a different sign than the Cr and Zn atoms: the spin up charge is lower than that corresponding to the minority spin component. Moreover, the polarization of the Se_1 atoms bonded with Cr is bigger than the Se_2 atoms.

The IB electrons are supposed to spend their time in regions (around the ions) where the presence of other particles would make them feel strong Coulomb repulsion, thus making their motion correlated. The band structure calculations are not the best approach to observe this physical behavior, as they are a manifestation of a one-body problem, whereas correlation is the result of many-body interactions. In order to analyze the correlation effects because of the IB, a further extension using the LSDA + U method is carried out to improve the description of the localized states.

Table 2. Energies (eV) for $U = 0$, 3, 6 and 9 eV. $\Delta E_{\mathrm{VI}}^{(+)}$, $\Delta E_{\mathrm{IC}}^{(+)}$ and $\Delta E_{\mathrm{I}}^{(+)}$ are the VB–IB gap, the IB–CB gap and the IB width for the majority spin component. $\Delta E_{\mathrm{VC}}^{(-)}$ is the VB–CB gap for the minority spin component and ΔE_{FI} is the Fermi energy with respect to the IB minimum.

U	$\Delta E_{\mathrm{VI}}^{(+)}$	$\Delta E_{\mathrm{IC}}^{(+)}$	$\Delta E_{\mathrm{I}}^{(+)}$	$\Delta E_{\mathrm{VC}}^{(+)}$	$\Delta E_{\mathrm{VC}}^{(-)}$	ΔE_{FI}
0	0.54	0.82	0.22	1.59	1.48	0.16
3	0.48	0.80	0.35	1.63	1.47	0.22
6	0.35	0.85	0.41	1.61	1.45	0.28
9	0.30	0.78	0.52	1.60	1.44	0.29

A weakness of the LSDA + U method is that U is an external parameter. We present the results as a function of U between 0 and 9 eV. The value obtained using theoretically constrained calculations [17] gives $U \sim 2.0$ eV. This value is within the interval $0 < U < 9$ eV analyzed in this work.

The gaps and bandwidths for $U = 0$, 3, 6 and 9 eV and the two spin components are shown in table 2. For the majority spin component $\Delta E_{\mathrm{VI}}^{(+)}$, $\Delta E_{\mathrm{I}}^{(+)}$, $\Delta E_{\mathrm{IC}}^{(+)}$, $\Delta E_{\mathrm{VC}}^{(+)}$ and ΔE_{FI} are the gaps between the VB maximum and the IB minimum, the IB bandwidth (the difference between the IB maximum and IB minimum), the gap between the IB maximum and the CB minimum, the gap between the VB maximum and the CB minimum ($\Delta E_{\mathrm{VC}}^{(+)} = \Delta E_{\mathrm{VI}}^{(+)} + \Delta E_{\mathrm{I}}^{(+)} + \Delta E_{\mathrm{IC}}^{(+)}$) and the Fermi energy with respect to the IB minimum. Similarly, $\Delta E_{\mathrm{VC}}^{(-)}$ is the gap between the VB maximum and the CB minimum for the minority spin component. As U increases from 0 to 9 eV, a decrease in $\Delta E_{\mathrm{VI}}^{(+)}$ and $\Delta E_{\mathrm{IC}}^{(+)}$, and an increase in the bandwidth $\Delta E_{\mathrm{I}}^{(+)}$, can be seen. The $\Delta E_{\mathrm{VC}}^{(+)}$ and $\Delta E_{\mathrm{VC}}^{(-)}$ gaps are lower than the experimental host semiconductor gap. However, it is necessary to point out that the LSDA + U method corrects the spurious self-interaction for the shells where it is applied, while the remaining ones are still affected by the self-interaction error. Therefore, when this self-interaction is corrected, the width of the IB will diminish and the gaps will increase. In this work, no correction for the band gap underestimation (upward shift) was made.

For all the U values, the total integrated DOS between the top IB and the Fermi energy is two electrons. The projected DOS for t, e and p orbital groups with $U = 3$, 6 and 9 eV are shown in figure 3. In all cases, the IB is mainly made up of the transition metal t orbitals, and with a lower proportion of the transition metal p orbitals. In all cases, the VB maximum also has a transition metal e orbital character. The contribution of all the orbitals within each group (t, e and p) is equal for $U = 0$ eV (figure 2). However, the situation is different for $U \neq 0$ eV, because the LSDA + U includes a spatial correlation degree associated with the anisotropy in the occupation numbers. It can be seen in figure 3 that all of the p, t and e orbitals are split into several contributions. Therefore, in general, the degeneration is broken and the contribution to projected DOS will be different because of the increase in U.

It can be seen in figure 3 that the contribution of the d_{xy} orbital for $U = 3$ and 6 eV is split with respect to the other t orbitals. For $U = 9$ eV the contributions of the three t orbitals are different. The orbital contribution has more structure with the increase in U. Moreover, the charge of these orbitals will be similar for $U = 0$ eV and for $U \neq 0$ eV, because the integrated DOS between the IB minimum and the Fermi energy is similar for all U values.

For $U = 0$ eV the contribution of the two e orbitals (d_{z^2} and $d_{x^2-y^2}$) is equal. However, an increase in U produces a different contribution to the projected DOS. The edge of the VB increases the d_{z^2} character slightly and decreases the $d_{x^2-y^2}$ character slightly. For these orbitals the modification of the charge with U is also small.

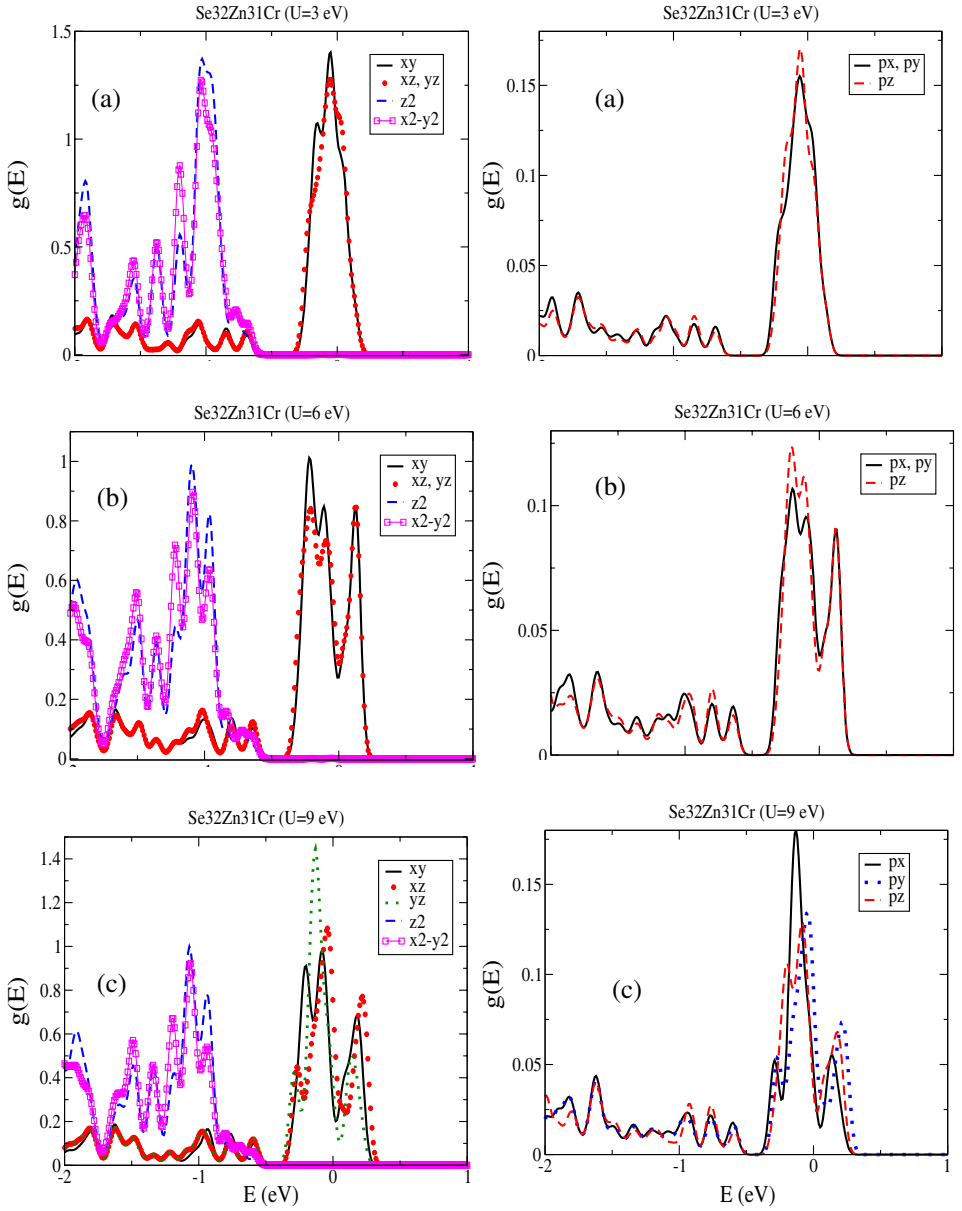

Figure 3. Projected DOS on d (left panels) and p orbitals (right panels) of the Cr atom with (a) $U = 3$ eV, (b) $U = 6$ eV and (c) $U = 9$ eV. The Fermi energy has been chosen as zero in this figure.

The variation in the contribution to the projected DOS of the transition metal p orbitals with U is similar to the contribution of the transition metal t orbitals. An increase in U splits the contribution to the IB. However, the effect on the p orbital charge is smaller than on the d orbitals because the contribution of the p orbitals to the IB is much smaller than the contribution of the d orbitals.

Generally, one would expect a substantial shift in the position of the empty Cr d bands in LSDA+U due to the local Coulomb interaction U. The Coulomb interaction induces almost no changes in the VB and the IB. The expected shift of the Cr d bands is indeed observed in the CB. It can be explained if we keep in mind two facts. Firstly, an analysis of the DOS and population analysis of the Cr d orbitals indicate that the t spin up component contributes principally to the VB and IB, the e spin up components contribute principally to the VB and the t and e spin down components contribute principally to the CB. Secondly, from the LSDA + U methodology, the energy of the monoelectronic levels is $\varepsilon^{(\sigma)}_{m\,[\mathrm{LSDA}+U]} = \varepsilon^{(\sigma)}_{m\,[\mathrm{LDDA}]} + U(1/2 - n^{(\sigma)}_{\mathrm{m}})$, where $n^{(\sigma)}_{\mathrm{m}}$ are the elements of the occupation number matrix for the spin σ. Therefore, the occupied and unoccupied orbitals are shifted by $-U/2$ ($n^{(\sigma)}_{\mathrm{m}} = 1$) and $U/2$ ($n^{(\sigma)}_{\mathrm{m}} = 0$) respectively, reproducing the correct physics of a Mott–Hubbard transition qualitatively. If a band is only formed by the m orbital, the previous qualitative reasoning is correct. However, if the contribution of the m orbital to the band is very small, then the split is also very small, or equivalently the effective U is reduced by combination of the m orbital with the host semiconductor. This explains the small shift in the IB because of the combination of the Cr t orbitals with the Se p orbitals. Moreover, as the t and e spin up components contribute principally to the VB and the spin down components contribute principally to the CB, the majority components experience a downward shift in the VB and the minority components and an upward shift in the CB. Therefore, from the results, the largest changes with respect to LSDA will be in the range of energy where the contribution of the Cr d orbital to the bands is larger. According to the results, this range of energy does not correspond to the IB. For this reason, it is not split.

A population analysis indicates that the charge variation for different U values and the variation between the orbitals of the same group (t, e and p) are very small, of the order of 10^{-2} times the electron charge. Therefore, the contribution to the projected DOS with U of the majority-spin Cr d bands (figure 3) remains largely intact and the changes in orbital occupancies are fairly small. The LSDA + U method usually favors complete occupancy of certain orbitals, while empty ones are shifted upwards in energy. However, in the present case, the 3d bands of t symmetry of the Cr atom remain uniformly occupied. As has been previously mentioned, this behavior is due to the Coulomb interaction inducing almost no changes in the occupied bands (the VB and partially the IB).

In order to analyze the charge distribution between different spin orientations, we have carried out a study of the system magnetization. The magnetization of the unit cell for all U values is 4 μ_{B}. The magnetic moments per atom for $U = 0$ are $m_{\mathrm{Cr}} \approx 4.40\ \mu_{\mathrm{B}}$, $m_{\mathrm{Se}_1} = -20.45 \times 10^{-3}\ m_{\mathrm{Cr}}$, $m_{\mathrm{Se}_2} = -1.56 \times 10^{-3}\ m_{\mathrm{Cr}}$ and $m_{\mathrm{Zn}} = +1.36 \times 10^{-3}\ m_{\mathrm{Cr}}$ respectively. However, the magnetization of the Cr atom increases from 4.40 μ_{B} for $U = 0$ eV to 4.48 μ_{B} for $U = 9$, and that of the Se_1 atoms decreases to $-22.27 \times 10^{-3}\ m_{\mathrm{Cr}}$ for $U = 9$ eV. For Se_2 and Zn atoms the variation is very small. When Cr is incorporated into ZnSe, two Cr electrons are given to the bonds, thus forming the deep impurity level $\mathrm{Cr}^{2+}(3\mathrm{d}^4)$. Using the free-ion model, the ground configuration is $^5\mathrm{D}_0$ according to Hund's rules. The crystalline field further splits this configuration into a multiplet of symmetry T_2 and a multiplet E. Therefore, the magnetic moment of the Cr atom in this alloy is lower than expected from the free-ion picture because of the overlap and the negative polarization of the Se atoms with respect to that of Cr.

In figure 4 we present the radial distribution of magnetization around the Cr and Se atoms for $U = 0$ and 9 eV. This radial distribution is the charge difference between the majority and minority spin orientations within a sphere of radius r, and depends on the radius r from the atom considered and the difference between the majority and minority charge densities. For Cr, the magnetization saturates around $r^{(\mathrm{Cr})}_{\mathrm{s}} = 2.0$ Å (the inset in figure 4(a)). For $r = 11.34$,

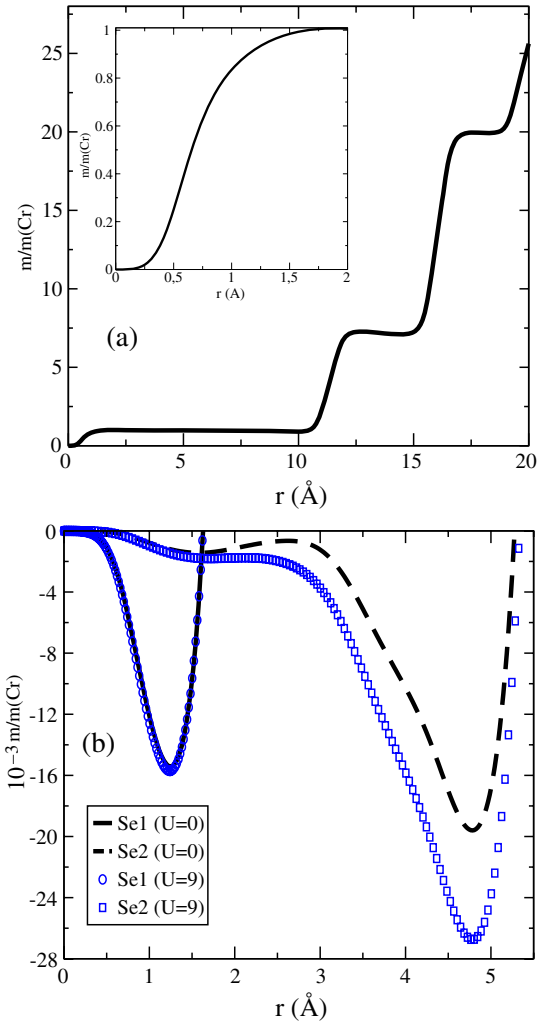

Figure 4. Radial distribution of magnetization within a sphere of radius r placed at (a) Cr and (b) Se_1 and Se_2 atoms with $U = 0$ and 9 eV. The Se_1 atoms are those directly bonded to the Cr atom and the Se_2 atoms are those which are not. The inset in (a) shows this distribution with a smaller range. The units of the radial distribution are scaled with respect to the saturation value of the Cr atom when $U = 0$ ($m_{Cr} = 4.40\ \mu_B$).

16.04 and 19.64 Å it has a great increase because of the six, 12 and eight Cr atoms placed at this distance from the origin. These increases are proportional to the number of Cr atoms in these positions with respect to the Cr atom taken as the origin.

In contrast, the radial magnetization around the Se_1 atoms (bonded with Cr) has a negative minimum around 1.2 Å, followed by a sharp increase (figure 4(b)). The small difference between the radial magnetizations of the Se_1 atoms for $U = 0$ and 9 eV is almost inappreciable in the figure. The Se_2 atom also shows this behavior (figure 4(b)), with a small minimum around $r = 1.5$ Å and a deeper minimum around $-20 \times 10^{-3}\ m_{Cr}$ for $r = 4.7$ Å. The increase in the depth of the second minimum when $U = 9$ eV is due principally to the decrease in the polarization of the Se_1 atoms at approximately 4 Å from the Se_2 atom.

According to recent results in materials with an IB, when LSDA + U and LSDA-SIC (LSDA with self-interaction correction) are used [8–10], the IB is maintained. The main effects of the LSDA + U corrections are a modification in the relative composition of the five transition metal d orbitals, a reduction of the VB–IB and IB–CB band gaps, a increase in the IB bandwidth and a reduction in the contribution of the transition metal d orbitals at the Fermi energy. It is interesting to note that the effect of the correlation when Cr substitutes a Zn atom in the ZnSe host semiconductor is lower than when the host semiconductor is ZnS [8]. In the latter, for values of U greater than 6 eV, the IB is split, thus creating two bands, a full one below the Fermi energy, and an empty one above it, i.e. a metal–insulator transition.

Scaling the thresholds of the two absorptions VB–IB ($E_1 = \Delta E_{\mathrm{VI}}^{(+)} + \Delta E_{\mathrm{FI}}$) and IB–CB ($E_2 = \Delta E_{\mathrm{VC}}^{(+)} - E_1$) with the quotient between the experimental and theoretical gaps, the values of E_1 and E_2 vary from 1.40 and 1.78 eV for $U = 0$ to 1.18 and 2.02 eV for $U = 9$ eV. These theoretical values compare well with the experimental ones (close to 1.4 and 2.2 eV [1]). These thresholds would be more similar to the experimental ones if a self-interaction correction were also included (GW and EXX methods) because the band gap underestimation and bandwidth overestimation would be corrected.

The acceptor and donor transition energy levels have also been calculated using total energy calculations in different charge states instead of monoelectronic energies. Because LSDA + U does not change the LSDA picture much these calculations have been done with $U = 0$. From these results, the donor and acceptor levels are 0.66 and 1.98 eV above the VB, in good agreement with the results of the literature (0.46 eV [18] and 1.93 eV [19]). One possible reason for this discrepancy is that the Cr concentration in our calculations is larger than that usually used in doped semiconductors.

Focusing on solar cells, an increase in the U-term brings about a decrease in efficiency because the IB bandwidth and Fermi energy change with respect to $U = 0$. The maximum efficiency is reached when a photon created by a radiative recombination from band X to band Y can only be reabsorbed in a transition from band Y to X [20]. Therefore, as U increases, this ideal process of recycling photons diminishes: a photon created by radiative recombination from IB (CB) to VB (IB) can be reabsorbed in a radiative transition either from the VB to the IB or from the IB to CB. However, this fact would increase the efficiency of other semiconductor devices, such as up- and down-converters, favoring only a certain transition.

4. Conclusions

In this work the electronic properties (bands, DOS, gaps, charges and electron densities) of ZnSe with Cr have been analyzed. This material presents an intermediate metallic band in the wide range of U values studied. A splitting of the occupied and empty IB states is not seen when the atoms are allowed to relax without any symmetry constraints. Nor it is observed when $U \leqslant 9$ eV. Because of the properties of this IB, the efficiency of the mid-infrared lasers, up- and down-converters and solar cells based on this material can be increased with respect to when the host semiconductor is used without Cr. Nevertheless, an increase in the U-term brings about a decrease in the efficiency of solar cells because the IB bandwidth and Fermi energy change. In the worst case, it could produce a metal–insulator transition and the material would not have a partially filled IB, but a full one below the Fermi energy and an empty one above it. This is not the case in the system analyzed here. The IB of this material is also more insensitive to the increase in self-repulsion and the relaxation of the atomic positions compared with other II–VI semiconductors doped with Cr.

Acknowledgments

The author gratefully acknowledges the computer resources, technical expertise and assistance provided by the Barcelona Supercomputing Center. This work has been supported by the GENESIS FW project of the National Spanish program CONSOLIDER (CSD2006-0004) and by La Comunidad de Madrid through the funding of the project NUMANCIA (reference no S-0505/ENE/0310).

References

[1] DeLoach L D, Page R H, Wilke G D, Payne S A and Krupke W F 1996 *IEEE J. Quantum Electron.* **32** 885
Kasiyan V A, Shneck R Z, Dashevsky Z M and Rotman S R 2002 *Phys. Status Solidi* **229** 395
[2] Tablero C 2005 *Phys. Rev.* B **72** 035213
Tablero C 2006 *Sol. Energy Mater. Sol. Cells* **90** 203
Tablero C 2006 *Sol. Energy Mater. Sol. Cells* **90** 588
Tablero C 2006 *Comput. Mater. Sci.* **36** 263
Tablero C 2005 *Solid State Commun.* **133** 97
Luque A and Martí A 2001 *Prog. Photovolt. Res. Appl.* **9** 73
Martí A, Cuadra L and Luque A 2000 *Proc. 28th IEEE Photovoltaics Specialists Conf.* vol 940 (New York: IEEE)
Yu K M, Walukiewicz W, Wu J, Shan W, Beeman J W, Scarpulla M A, Dubon O D and Becla P 2003 *Phys. Rev. Lett.* **91** 246403
[3] Luque A and Martí A 1997 *Phys. Rev. Lett.* **78** 5014
[4] Shockley W and Queisser H J 1961 *J. Appl. Phys.* **32** 510
[5] Hohenberg P and Kohn W 1964 *Phys. Rev.* B **136** 864
[6] Martin R M 2004 *Electronic Structure. Basis Theory and Practical Methods* (Cambridge: Cambridge University Press)
Ohno K, Esfarjani K and Kawazoe Y 1999 *Computational Materials Science. From Ab Initio to Monte Carlo Methods* (Berlin: Springer)
Parr R G and Yang W 1989 *Density Functional Theory of Atoms and Molecules* (Oxford: Oxford University Press)
Dobson J F, Vignale G and Das M P 1998 *Electron Density Functional Theory: Recent Progress and New Directions* (New York: Plenum)
[7] Anisimov V I, Aryasetiawan F and Lichtenstein A I 1997 *J. Phys.: Condens. Matter* **9** 767
Anisimov V I, Zaanen J and Andersen O K 1991 *Phys. Rev.* B **44** 943
Dudarev S L, Botton G A, Savrasov S Y, Humphreys C J and Sutton A P 1998 *Phys. Rev.* B **57** 1505
[8] Tablero C 2005 *J. Chem. Phys.* **123** 114709
[9] Tablero C 2005 *J. Chem. Phys.* **123** 184703 The code used is a private modification of SIESTA code [12] where the author has implemented the DFT + U method
[10] Wierzbowska M, Sánchez-Portal D and Sanvito S 2004 *Phys. Rev.* B **70** 235209
Filippetti A, Spaldin N A and Sanvito S 2005 *Chem. Phys.* **309** 59
Sandratskii L M, Bruno P and Kudrnovsky K 2004 *Preprint* cond-mat/0404163
[11] Kohn W and Sham L J 1965 *Phys. Rev.* **140** A1133–8
[12] SIESTA code: Soler J M, Artacho E, Gale J D, García A, Junquera J, Ordejon P and Sánchez-Portal D 2002 *J. Phys.: Condens. Matter* **14** 2745
Artacho E, Sánchez-Portal D, Ordejón P, García A and Soler J M 1999 *Phys. Status Solidi* b **215** 809
Sánchez-Portal D, Artacho E and Soler J M 1997 *Int. J. Quantum Chem.* **65** 453
Ordejón P, Artacho E and Soler J M 1996 *Phys. Rev.* B **53** R10441
[13] Ceperley D M and Alder B J 1980 *Phys. Rev. Lett.* **45** 566
[14] Troullier N and Martins J L 1991 *Phys. Rev.* B **43** 1993
[15] Kleinman L and Bylander D M 1982 *Phys. Rev. Lett.* **48** 1425
Bylander D M and Kleinman L 1990 *Phys. Rev.* B **41** 907
[16] Sankey O F and Niklewski D J 1989 *Phys. Rev.* B **40** 3979
[17] Dederichs R H, Bltigel S, Zeller R and Akai H 1984 *Phys. Rev. Lett.* **53** 2512
Solovyev I V, Dederichs R H and Anisimov V I 1994 *Phys. Rev.* B **50** 16861
Pickett W E, Erwin S C and Ethridge E C 1998 *Phys. Rev.* B **58** 1201

[18] Godlewski M and Kaminska M 1980 *J. Phys. C: Solid State Phys.* **13** 6537
Kasiyan V A, Shneck R Z, Dashevsky Z M and Rotman S R 2002 *Phys. Status Solidi* **229** 395
Rablau C I, Ndap J O, Ma X, Burger A and Giles N C 1999 *J. Electron. Mater.* **28** 678
[19] Grebe G, Roussos G and Schulz H J 1976 *J. Phys. C: Solid State Phys.* **9** 4511
Bhaskar S, Dobal P S, Rai B K, Katiyar R S, Bist H D, Ndap J-O and Burger A 1999 *J. Appl. Phys.* **85** 439
[20] Luque A, Marti A and Cuadra L 2000 *Proc. Conf. on 16th European Photovoltaic Solar Energy* ed W G Madow (London: James and James) pp 59–61